Alkyl Chain Dynamics in Monolayer-Protected Clusters (MPCs): A Quasielastic Neutron-Scattering Investigation

S. Mitra,[†] Binoj Nair,[‡] T. Pradeep,*[,‡,⊥] P. S. Goyal,[§] and R. Mukhopadhyay*[,†,∥]

Solid State Physics Division, Bhabha Atomic Research Centre, Trombay, Mumbai 400 085, India, Department of Chemistry and Regional Sophisticated Instrumentation Centre, Indian Institute of Technology, Madras 600 036, India, and Inter-University Consortium for DAE facilities, BARC, Mumbai 400 085, India

Received: December 5, 2001; In Final Form: January 10, 2002

Dynamics of alkyl chains in an isolated monolayer protected cluster (MPC), AuC_{18} (C_n = *n* carbon *n*-alkanethiolate), and a superlattice of AgC_8 MPC have been investigated by quasielastic neutron scattering (QENS) technique in the temperature range of 300−400 K. The results have been compared with a layered silver thiolate, AgC_{12}, chosen to represent a planar two-dimensional monolayer. In the cluster superlattice, QENS broadening was observed even at room temperature and below the chain melting temperature (T_{cm}) whereas for the isolated cluster it was seen only above T_{cm}. In the layered silver thiolate, it was observed above the melting point. Data pertain to the rotational motions of the alkyl chains and can be best described by jump diffusion among *N* equivalent sites or continuous rotation about the molecular axis. At room temperature, the observed dynamics in AgC_8 correspond only to the noninterdigitized molecular chains which amount to about 50% of the total. Above 340 K, contribution from the interdigitized chains manifest and at 380 K, close to the superlattice melting, all the chains become dynamic. It is clearly established that the temperature required for the dynamics to manifest increases from the isolated cluster to the superlattice to the thiolate, suggesting a gradual increase in intermolecular interactions. Reorientation times for all these systems have been obtained at each temperature.

I. Introduction

The study of structure and properties of ultrathin films at interfaces has advanced at a rapid pace with their potential applications in the fields of optoelectronics and molecular engineering.[1] These ordered films have been classified into Langmuir−Blodgett films[2] and self-assembled monolayers (SAMs),[3] the molecular assemblies, which form spontaneously by immersion of an appropriate substrate into a solution of active surfactant. The classification of the structure and properties of SAMs is based on the dimensionality, i.e., two-dimensional (2D) SAMs and three-dimensional (3D) SAMs. The 2D SAMs are ordered molecular assemblies formed by the adsorption of an active surfactant on a planar solid substrate.[4] Most of the alkanethiolate SAMs have been prepared on the Au (111) face.[5] The 3D SAMs are monolayers of surfactants formed on a nanosized metal core, the whole system together is called the monolayer protected metal clusters (MPCs). The core of this system consists of dense-sphere packing of metal atoms resulting in nanocrystals with specific lattice planes on the surface and the alkylthiolates are adsorbed on these lattice planes.[6] The monolayers on the metal core substrate are similar to monolayers on 2D SAMs. The large surface area of the clusters helped in studying the properties, structure and dynamics of the monolayers using bulk techniques such as ^{13}C NMR[7a,b] and transmission IR[7c] spectroscopies which are impossible in the case of 2D SAMs owing to poor number density of the species concerned. Despite this limitation, dynamics studies have been performed on planar monolayers.[8] In Figure 1, a schematic of a monolayer protected cluster is shown.

In 3D SAMs, the surface alkyl chains diverge as they move away from the core, resulting in the interpenetration of the monolayers of adjacent clusters in the solid state. Such interactions between isolated monolayer chains or bundles of chains lead to the formation of crystalline solids of the clusters called superlattices (Figure 1). Superlattices are identical to molecular crystals, they are recrystallizable from solutions of isolated clusters.[9] Interdigitation between alkyl chains give strong intercluster interactions and the superlattices are stable even above the alkyl chain melting temperature. However, the individual clusters separate at still higher temperatures. Alkyl chains with less than five carbon atoms are less ordered and these clusters do not show interdigitation and the solid does not show superlattice order. Clusters with longer chain monolayers are more ordered with less gauche defects. Interdigitation is more and there is superlattice formation.

The present study was undertaken with the objective of understanding the dynamics of alkyl chains in the isolated MPCs and metal cluster superlattices, especially when they go through a phase transition. The systems chosen are octadecanethiol capped gold cluster (AuC_{18}) and octanethiol capped silver cluster (AgC_8), while the monolayer assembly around the cluster in the former is near perfect with all-trans conformation, the latter exhibits a superlattice assembly. X-ray diffraction study shows that AgC_8 is essentially a single phase superlattice.[10−12] The superlattice diffractions were observed up to 398 K indicating the absence of phase transitions. However, at 423 K the superlattice peaks are absent; individual cluster peaks dominate

* To whom correspondence should be addressed.
[†] Solid State Physics Division.
[‡] Department of Chemistry and Regional Sophisticated Instrumentation Centre.
[§] Inter-University Consortium for DAE facilities.
[⊥] E-mail: pradeep@iitm.ac.in. Fax: ++91-44-235-0509/2545.
[∥] E-mail: mukhop@apsara.barc.ernet.in. Fax: +91-22-5505151.

10.1021/jp0144146 CCC: $22.00
Published on Web 00/00/0000 PAGE EST: 7.2

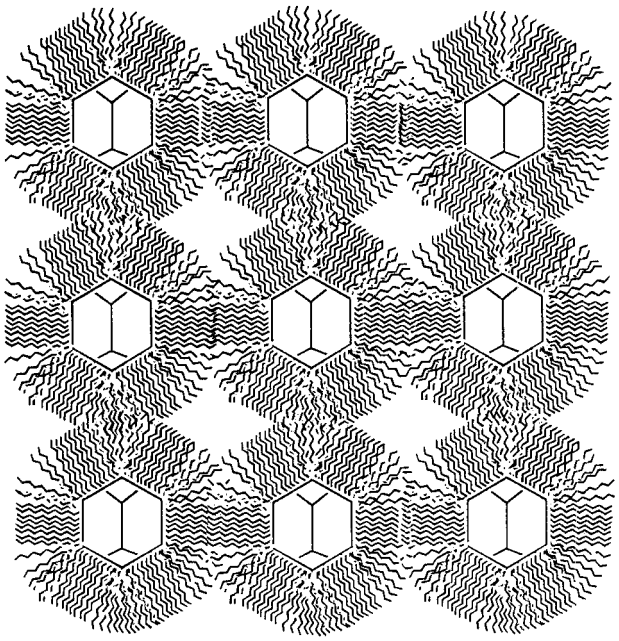

Figure 1. Schematic of a monolayer protected cluster (MPC) and the cluster superlattice. The hexagonal structure represents the metal cluster core and the wiggles are the monolayers. The diameter of the metal core is in the range of 30 Å and the thickness of the monolayer investigated here is in the range of 12−29 Å. The molecules adsorb on the specific lattice planes on the surface of the metal nanocluster (depicted as cuboctahedrons). Alkyl chains are seen diverging as they move away from the core. Interdigitation among individual clusters is seen principally along the unit cell axes. Part of the alkyl chain assembly may be disoriented.

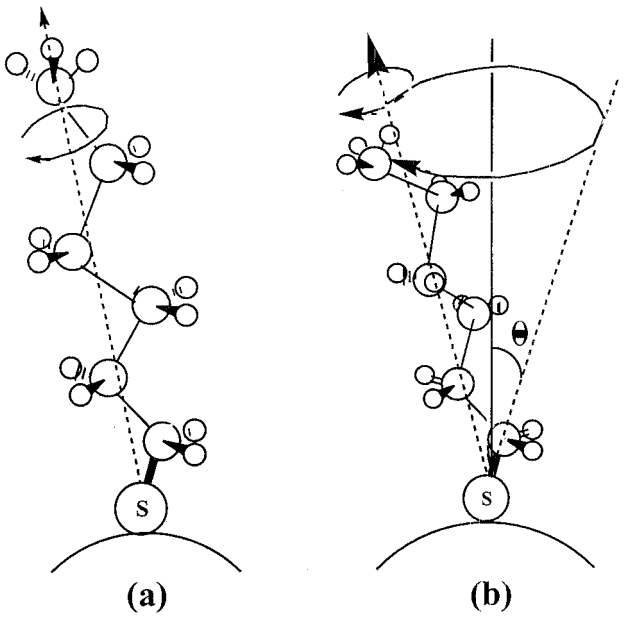

Figure 2. (a) Rotational dynamics where alkyl chains rotate about its central axis. (b) Rotational dynamics involving precessional motion with a cone angle, Θ. Sulfur atom is at the apex of the cone, firmly fixed on the metal core. The dynamics are maximum at the alkyl chain terminus and minimum closest to the core.

at 448 K. At 473 K, intensities of (111) and (200) peaks of Ag increase and beyond 473 K the pattern remains unchanged. Upon cooling from high temperature (>473 K), the superlattice patterns are not seen suggesting that material does not regain the superlattice order. However, cooling from a lower temperature of 450 K regains the superlattice order. The DSC experiments however, show two consecutive phase transitions. The broad peak in the range of 315−340 K is related to *alkyl chain melting*, and a peak in the range of 375−400 K is related to *superlattice melting*. The peak due to alkyl chain melting is at 339.7 K and that due to superlattice melting is seen at 399.2 K. Both XRD and DSC show the reversibility of superlattice transition at lower temperatures and irreversibility at higher temperatures.

Au clusters are not ideal candidates for superlattice formation, as shown in earlier studies.[10−12] No superlattice structure is found in XRD for AuC_{18}. In accordance with that only a very weak transition is seen in DSC corresponding to superlattice melting, but a large enthalpy change is seen for alkyl chain melting. The first transition due to alkyl chain melting is observed at 333.5 K. Infrared signatures for the melting transition are similar as in the case of AgC_8. The chain melting temperature does not seem to depend very much on the chain length as similar DSC and IR features are seen for AuC_8.

The alkyl chain assembly in layered silver thiolate[13−15] is similar to that in planar SAMs. Only one transition at about 400 K is observed in the DSC experiment. X-ray diffraction shows vanishing Bragg peaks above 400 K and these peaks were found to reappear on lowering the temperature. Variable temperature IR studies show change in modes with increase in temperature indicating melting from the crystalline phase to a liquid phase. This transition is at a higher temperature than the cluster superlattices indicating that van der Waals attraction is stronger in the case of thiolates. Presence of all-trans conformations is seen in IR indicating more order. As in the MPCs, T_{cm} does not depend on the chain length. Many structural and spectroscopic insights into the structure of cluster solids can be derived from a comprehensive study of thiolates. It may be added that melting of superlattices was studied using molecular dynamics methods.[16]

The phase transitions observed in these systems could be understood better in terms of the creation and propagation of dynamics in the alkyl chain assembly. These dynamics would depend on various parameters such as the length of the alkyl chain, intermolecular interaction, nature of metal substrates, temperature, and the structure and dimensionality of SAMs. Increased interpenetration of alkyl chains into one another would increase the packing density and hence restricts the dynamics. A crude model of dynamics is one in which molecular chains rotate about an axis. The rotations are restricted in the solid state, when surface coverage and packing density of alkanethiolates is high (C_n, $n > 5$). The next possibility is to have a precession of the alkyl chains with rigid sulfur atoms as the cone apex, which in turn is fixed on the metal core. The alkyl chains would perform a revolution with a cone angle which would depend on the free volume space for revolution and this motion would be controlled by inter and intramolecular interactions. These dynamics are expected when the alkanethiol coverage on the metal substrate is less. This can also occur at the lattice plane junctions on the cluster core surface where there is availability of free volume space. The dynamics of the terminal part of the alkyl chain would be maximum and negligible at the C−S region, which is firm on the substrate. The complexity of the dynamics would increase with intrachain rotations. The latter type of motions would be absent in case of thiolates where packing density is high. The various rotational dynamics possible for the alkyl chains are shown in Figure 2. The simple geometry of dynamics conceivable for the alkyl chain could be the axial rotation and the rotations about a cone angle. Cone angle tending to zero reduces the latter to the axial rotation and from simple calculation of moment of inertia, it

can be shown that even for a small cone angle of 20 deg, this motion requires much more energy—about 5 times—compared to the axial motion. In other words, the simplest dynamical motion would be the axial rotation of the alkyl chains. We report here the very first studies of dynamics of monolayers on clusters using neutron quasielastic scattering technique. There exist some neutron scattering studies investigating the vibrational and structural aspects in similar kind of nanoparticles and colloids[17−20] but no report is available on QENS measurements. The systems are chosen such that the similarities and differences between the alkyl chain dynamics of 2D and 3D monolayers as well as cluster superlattice assemblies are brought out. We are aware that a range of monolayer lengths can reveal more complete information: such studies are currently underway.

Neutron scattering is a powerful technique[21] to study the dynamics in condensed matter, as the energy of thermal neutrons match with the energy of the system. Further, systems containing protons are more suitable for neutron scattering studies for its large scattering cross section. The random motion of the particles in the system leads to Doppler broadening of the scattered neutrons which finally results in the broadening of the elastic line known as quasielastic neutron scattering (QENS). The QENS not only provides the time scale but also the geometry of motions. There are many examples where QENS technique has been successfully used to elucidate the molecular motions and physical properties related to them.[21−24] These properties make the QENS technique a unique tool to study the dynamics of alkyl chains in the monolayer assembled solids.

Following section gives the details of the experiment, the theoretical aspects and results are discussed in section III, and conclusion is given in section IV.

II. Experimental Details

The synthesis methodology is given below. Silver nitrate (Merck, 99.99%), chloroauric acid ($HAuCl_4 \cdot 3H_2O$, CDH, 99.8%), tetra *n*-octylammoniumbromide (Merck, 98%), sodium borohydride, octadecanethiol, octanethiol, and dodecathiol (all Aldrich, 99%) were used as received. Toluene and methanol used were analytical reagent (AR) grade. Deionized and distilled water were used for synthesis. For the synthesis of AgC_8, 0.0358 M toluene solution (21.6 mL) of tetra-*n*-octylammoniumbromide were added to vigorously stirred 0.0288 M (10 mL) of aqueous solution of silver nitrate. After 1 h of stirring, a 0.0139 M toluene solution (23.8 mL) of octanethiol was added. To this 8.25 mL aqueous solution (0.2378 M) of sodium borohydride was added dropwise. Reduction of silver was evidenced by brown color of the toluene phase. The solution was stirred overnight and organic layer was separated. It was allowed to evaporate slowly to 10 mL and 100 mL methanol was added to precipitate the cluster. The material was washed several times to remove the unreacted thiols and was finally air-dried. The product obtained was a fine brown powder. The same procedure was repeated for AuC_{18} using chloroauric acid and octadecanethiol instead. The product obtained was a black powder. For Ag-dodecathiolate (AgC_{12}), 0.0139 M toluene solution (47.6 mL) of dodecanethiol was added to 0.0288 M aqueous solution (20 mL) of silver nitrate and was stirred for 3 h. A white suspension was formed in the toluene layer, which was separated and centrifuged. The precipitate was washed with toluene and air-dried. The product obtained was a white crystalline powder. All syntheses were performed in covered flasks and the materials were stored in brown bottles due to possible light sensitivity. The synthesis had to be repeated several times to obtain adequate quantities of materials for neutron diffraction measurements. Apart from other reasons, the yield obtained in synthesis was one of the criteria for the selection of these systems. Within the temperature range studied, the samples were stable.

Neutron quasilelastic scattering experiments were carried out using the medium resolution quasielastic spectrometer[25] at Dhruva reactor at Trombay. The spectrometer is installed at the end of a through tube going through the reactor core. It has a double monochromator for variation of incident energy and an air cushion based spectrometer for energy analysis. A double monochromator placed inside the pile block of the reactor, provides a closer approach to the source. Vertically bent crystals[26] are used to focus the neutrons at the sample position and thereby enhance the neutron intensity substantially. The analyzer is used in Multi Angle Reflecting X-tal (MARX)[27] mode. Spectrometer in MARX mode essentially uses a combination of large analyzer crystal and a position sensitive detector, providing larger throughput. This is very much essential for such experiments to be carried out in a medium flux reactor. Pyrolytic graphite crystals are used for both the double monochromators and the analyzer. In the present configuration, the spectrometer has an energy resolution of 200 μeV with an incident wavelength of 4 Å. The quasielastic spectra were recorded in the wavevector transfer ($Q = 4\pi \sin\theta/\lambda$, where θ is the scattering angle, and λ is the wavelength of the incident neutron) range of 0.8 to 1.8 $Å^{-1}$. Sample, contained in a sachet of aluminum foil of ~1 mm thickness was placed at an angle bisecting the incident and the scattered beam. The sample thickness was chosen in order to minimize the multiple scattering effects. QENS measurements were carried out for AuC_{18} in the temperature range 300−360 K. The temperature ranges were 300−380 K for AgC_8 and 300−400 K for AgC_{12}. Samples were heated from both the sides using strip-type heaters fixed on the sample holder and the temperature was measured at top of the sample. The temperature was stable within ±1 K.

III. Results and Discussion

In the present systems, the hydrogen atoms are attached to the alkyl chains and the chains are fixed on the metal core, therefore no translational motion of the hydrogen atoms is expected. The observed dynamics in the QENS measurements should be related to the rotational motion of the alkyl chains only. In hydrogenous materials, the neutron incoherent scattering cross section from hydrogen atoms dominates over all the other scattering processes. The incoherent scattering law for rotational motion can be written as[21,22]

$$S_{\mathrm{inc}}(Q,\omega) \propto A(Q)\delta(\omega) + [1 - A(Q)]L(\Gamma,\omega) \qquad (1)$$

where the first term is the elastic part and second term is the quasielastic part. $L(\Gamma\omega)$ is a Lorentzian function, $L(\Gamma,\omega) = {}_1/_{\pi}{}^{\Gamma}/_{(\Gamma^2 + \omega^2)}$, and Γ is the half width at half-maximum (hwhm). Γ is inversely proportional to the characteristic time, τ, of the motion.

It is convenient to analyze the data in terms of elastic incoherent structure factor (EISF), which provides information about the geometry of the molecular motions. The EISF is defined[21] as

$$\mathrm{EISF} = \frac{I_{\mathrm{el}}(Q)}{I_{\mathrm{el}}(Q) + I_{\mathrm{qe}}(Q)} \qquad (2)$$

where, $I_{\mathrm{el}}(Q)$ and $I_{\mathrm{qe}}(Q)$ are the elastic and quasielastic intensities, respectively. $A(Q)$ in eq 1 is therefore nothing but the EISF.

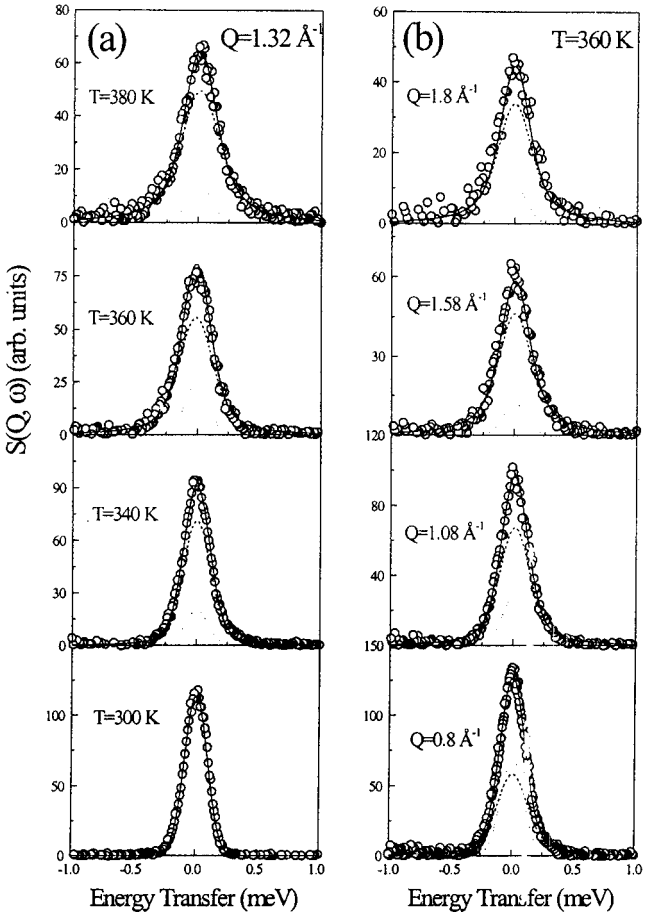

Figure 3. Typical QENS spectra for an isolated nonolayer protected cluster, AuC_{18}, (a) at Q = 1.32 Å^{-1} and at different temperatures (b) at 360 K, but at different *Q* values. Dashed and the dotted lines are the quasielastic and elastic components, respectively.

Analysis of the QENS data involves convolution of the theoretical scattering function with the resolution function of the instrument and determination of the different parameters characterizing the dynamical motion by least-squares fit with the measured data. These parameters need to be consistent at all the *Q* values and at all the temperatures for a describable model. The instrumental resolution function is measured independently using a standard vanadium sample and it is described quite well by a Gaussian function.

As mentioned above, we have studied isolated MPCs, superlattice MPCs in the class of 3D SAMs, and a layered system having molecular assembly similar to 2D SAMs.[15] The results pertaining to each of these systems are described below.

AuC_{18}. QENS data were recorded at room temperature (300 K), i.e., below the chain melting temperature, 340, 360, and 380 K. No quasielastic (QE) broadening was observed at 300 K indicating the absence of dynamical motion, at least within the time window of the instrument. However, at 340 K, QENS broadening was observed and so also at 360 and 380 K. The observation of QE broadening above 333 K is in conjunction with the DSC data and should be due to the dynamics of the alkyl chains. The QENS spectra as obtained for AuC_{18} at different temperatures and *Q* values are shown in Figure 3. While cooling the sample, the broadening continued to be observed below $T_{cm.}$ QE broadening was observed even at 300 K, although reduced in magnitude, indicating hysteresis in the sample.

At the first instance, we tried to separate the elastic and quasielastic contributions in the total spectrum using eq 1 without assuming any specific model and tried to choose the model suitable to describe the dynamics in the system under consideration. There are only two parameters in the eq 1 to be obtained from the fitting, *A(Q)* and Γ, HWHM of the Lorentzian function. As mentioned above, *A(Q)* is known as the EISF, providing information about the geometry of the motion and Γ is inversely proportional to τ, the time scale of the motion. In Figure 3 the dotted and dashed lines show the separated elastic and quasielastic components, respectively.

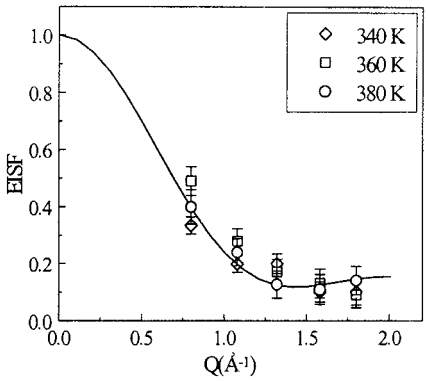

Figure 4. EISF as obtained for AuC_{18} at 340 and 360 and 380 K. The solid line corresponds to a model in which a particle performs random jumps among $N = 6$ equivalent sites on a circle with radius, *a* equal to 2.1 Å.

The extracted EISFs for AuC_{18} at 340 and 360 K are shown in Figure 4. To understand the dynamics further, one has to compare with different models. The models envisaged to describe the dynamics are (1) jump diffusion among N equivalent site on a circle, (2) uniaxial rotation: continuous rotation of the molecule about a fixed axis, and (3) isotropic rotation on a sphere of certain radius without any fixed axis.

In jump model among *N* equivalent sites on a circle, it is assumed that the motion is specified by jumps of certain angle and a characteristic time, τ. It is also assumed that the jump time is very much shorter than the time taken by the particle at a particular site, i.e., jumps are instantaneous and time taken at a particular site, τ is known as residence time. For a particle, which is allowed to perform a random jump among *N* equivalent sites on a circle, in which jumps are restricted to neighboring sites only, the expression of the scattering law for a powder sample[21,28] is

$$S(Q, w) = A_0(Q)\delta(\omega) + \sum_{l=1}^{l=N-1} A_l(Q)\frac{1}{\pi}\frac{2\tau^{-1}\sin^2\left(\frac{\pi l}{N}\right)}{\left[2\tau^{-1}\sin^2\left(\frac{\pi l}{N}\right)\right]^2 + \omega^2} \quad (3)$$

with

$$A_l(Q) = \frac{1}{N}\sum_{n=1}^{n=N} j_0(Qa_n)\cos\left(\frac{2ln\pi}{N}\right) \quad (4)$$

The a_n's are the jump distances under the effect of $(2n\pi/N)$ rotations and can be written as $a_n = 2a\sin(n\pi/N)$, where *a* is the radius of the circle. The correlation times can be evaluated as $\tau_l^{-1} = 2\tau^{-1}\sin^2(\pi l/N)$.

In case of uniaxial rotational diffusion model, molecular reorientation is assumed to take place continuously, in a circle of radius *a*. It has been shown by Dianoux et al.[29] that the incoherent scattering law for a scattering particle undergoing

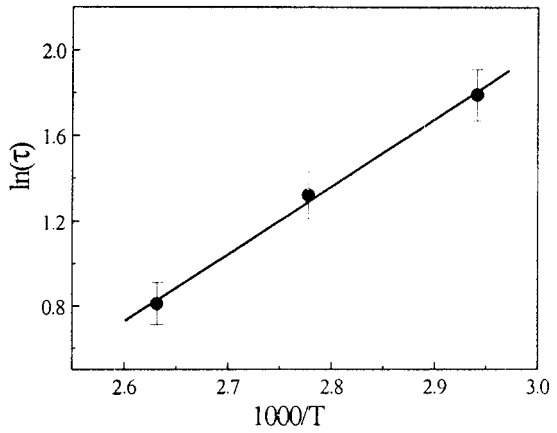

Figure 5. Arrhenius plot of ln(τ) vs 1000/T for AuC_{18}.

TABLE 1: Reorientation Time as Obtained for Different Systems and at Different Temperatures

	τ (ps)		
T (K)	AgC_8	AuC_{18}	AgC_{12}
300	5.2 ± 0.7		
340	3.7 ± 0.4	6.2 ± 0.7	
360	2.9 ± 0.3	3.7 ± 0.4	
380	4.1 ± 0.5	2.3± 0.3	
400			3.8 ± 0.4

uniaxial rotational diffusion on the circle of radius a, will depend on the angle θ between scattering vector $\boldsymbol{Q}$ and the rotation axis. It may be noted that the structure factor with jump diffusion model for $N \geq 6$ becomes indistinguishable from the uniaxial rotational diffusion model in the Q range of the present experiment.

In isotropic rotational diffusion model,[30] the molecule can perform continuous rotational motions on a sphere of radius r, with a diffusion constant, D_r, and thus has no fixed axis of rotation. This model may be ruled out from the geometry of the system, the chains are fixed on the surface of the cluster, so rotation about any axis is not possible.

Uniaxial rotation and jump diffusion for large N lead to the same structure factor, therefore it will be difficult to distinguish these two models for large N ($N \geq 6$). It is found that the radius of gyration equal to 2.1 (±0.1) Å gives the best fit to the experimentally obtained EISF within a 6-fold jump model. The solid line in Figure 4 is the calculated EISF. The model $S(Q,\omega)$, assuming a 6-fold jump diffusion model with radius of gyration 2.1 Å, was found to give very good fit to the data over the whole Q and temperature range. This demonstrates the applicability of the model to describe the dynamics of the alkyl chains in AuC_{18}. The estimated residence times at different temperatures are given in Table 1. The activation energy (E_a) of the rotation was determined from the τ Vs. temperature plot, using the Arrhenius Law, $\tau = \tau_0 e^{E_a/KT}$(Figure 5). An E_a of 6.3 ± 0.4 kcal/mol has been obtained.

The finding that the radius of gyration is 2.1 (±0.1) Å is significant. For closest contact distance of alkyl chains, the radius is 2.12 Å. The fact that the nearest neighbor distance in planar monolayers is greater than the shortest contact distance (4.24 Å), makes the chains to bend with an angle of ~30° in them. The conclusion that the alkyl chains occupy a space very similar to their nearest contact distance implies that the chains are erect and all-trans. This can happen only if the alkyl chains form columns on the lattice planes on the nanocrystals.

AgC_8. AgC_8, is a monolayer capped metal cluster, exhibiting superlattice structure. To investigate the dynamics in this system,

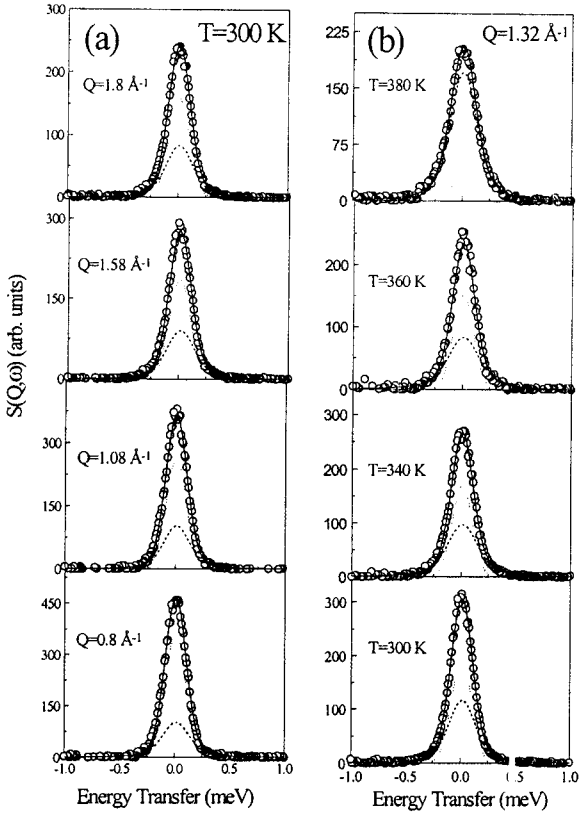

Figure 6. Typical QENS Spectra for monolayer protected cluster superlattice, AgC_8, (a) T = 300 K, but at different Q values, (b) Q = 1.32 Å^{-1} at different temperatures. Dashed and the dotted lines are the quasielastic and elastic components, respectively.

QENS spectra were recorded at RT, 340, 360, and 380 K. Although DSC experiments showed transitions corresponding to the chain melting at 339 K, surprisingly, even at room temperature, QE broadening was observed indicating the presence of dynamical motion in AgC_8. The QENS spectra as obtained from AgC_8 at different Q values at *RT* are shown in Figure 6a. Quasielastic broadening continued to observe with different degree at higher temperatures as well. Typical spectra at Q = 1.32 Å^{-1} and at different temperatures are shown in Figure 6b. It may be noted that both the alkyl chain melting (315−340 K) and the superlattice melting (375−400 K) are diffuse in nature as observed in the DSC experiments. The feature at and around 340 K will not be related to the superlattice melting. However, at 380 K, there could be an influence of the same. We shall discuss below the details of the dynamics as observed at each temperature.

As before, in the first instance, the elastic and QE components were separated using eq 1 and then the EISF was extracted as per eq 2. The variation of EISF with Q at different temperatures is shown in Figure 7. The fits reproduce the changes qualitatively and are considered very good as per QENS standards. It is clear that the EISF behaves differently with temperature unlike the case of AuC_{18}. Particularly, at *RT* and 340 K, the EISF is saturated at Q = 1 Å^{-1} itself. EISF is the measure of the elastic component in the total spectrum. Large EISF means, less quasielastic component, which implies that the contribution to the dynamics is less and vice-versa. This was not the case in AuC_{18} indicating possibility of partial dynamics in AgC_8. It can then be concluded that all the protons are not in motion or frozen. If there are some protons not undergoing any motion, they will contribute to the elastic scattering only. In that case, the generalized scattering law can be written as

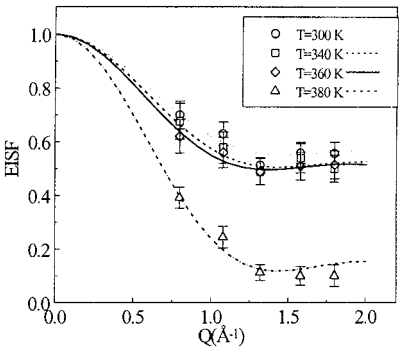

Figure 7. EISF for AgC_8, as extracted from the measured $S(Q,\omega)$ at different temperatures. The lines correspond to the model in which a particle performs random jumps among $N = 6$ equivalent sites on a circle (see text).

$$S(Q,\omega) = (1 - p_x)\delta(\omega) + p_x\,[A_0\delta(\omega) + (1 - A_0)L(\omega,\Gamma)] \quad (5)$$

where p_x is the fraction of hydrogen atoms in the system participating in the dynamics. A_0 is the EISF as described above and will depend on the model. The first term in the right-hand side is the elastic contribution from the static hydrogen atoms in the total spectrum whereas second term is weighted with the fraction of hydrogen atoms in the alkyl chains participating in rotational motion. The total elastic fraction can be written as

$$\mathrm{EISF_{Tot}} = [p_x A_0 + (1 - p_x)] \quad (6)$$

Assuming the same model of uniaxial rotation or jump diffusion among $N = 6$ equivalent sites as found to best describe the rotational dynamics of the alkyl chains in AuC_{18}, we attempted to determine p_x by least-squares fit of the extracted EISF from the experimental data using eq 6. It may be noted that the EISF also depends on the radius of gyration and was kept as a parameter in the least-squares fit. The parameters, fraction of mobile protons and the radius of gyration obtained at different temperatures are given in Table 2. It is found that at room temperature about 50% of the chains are contributing to the dynamics. This is not surprising and is understood by the following argument. AgC_8 forms a superlattice structure and this is by virtue of the chain interdigitation among the neighboring clusters. The number of chains or fraction of chains interdigitating would depend on the structure. For a simple cubic lattice and assuming nearly spherical cluster geometry (actually truncated icosahedron), only those chains along the unit cell axes will be interdigitating. That would permit only around half the chains to be free and others interact quite strongly. At 340 K EISF is found to be lower indicating that more protons start contributing to the dynamics. The value of p_x was 0.56 at 340 K. Similar picture sustains at 360 K and p_x becomes 0.57. It may be noted that DSC measurement[11,12] showed transition corresponding to the chain melting above 333 K. Therefore, the present observation is in conjunction with DSC. However at 380 K, the EISF shows a drastic change. The obtained value of p_x of 1 suggests that almost all the chains are contributing to the dynamics. This being closer to the melting point, the chains, which were earlier held fixed due to interdigitation, now have enough energy to be dynamic. The chains which were participating in the interdigitation and not dynamic at lower temperatures are now contributing to the observed dynamics but are slower than the others which do not participate in interdigitation. It is also found that data correspond to a model in which the hydrogen atoms of the alkyl chains are lying, on the average,

TABLE 2: Parameters, Fraction of Mobile Protons, p_x and the Radius of Gyration, a, as Obtained from the Least Squares Fit of the EISF Assuming a 6-Fold Jump Diffusion Model at Different Temperatures for AgC_8.

T (K)	p_x	a
300	0.50 (±0.02)	2.0 (±0.1)
340	0.56 (±0.02)	2.0 (±0.1)
360	0.57 (±0.01)	2.1 (±0.1)
380	1.00 (±0.02)	2.0 (±0.1)

on the surface of a cylinder of radius of about 2.1 Å. This structure is in accordance with alkyl chain packing as mentioned above. The model $S(Q,\omega)$ assuming 6-fold jump diffusion model with different radius of gyration (a) and quasielastic fraction (p_x) as given in Table 2 was found to give a very good fit to the data over the whole temperature range. The residence times obtained at different temperatures are given in Table 1.

The temperature dependence of the residence time is supposed follow Arrhenius Law; however, we find here that it is not so. This unusual behavior can be understood by the fact that the above residence times are actually effective ones, resulting from the combination of residence times of two dynamically different rotating units. One corresponds to the noninterdigitized alkyl chains that contribute even at 300 K (and at 340 K as well), while the other one corresponds to interdigitized alkyl chains, which contributes only above 340 K. Since the motion of the later unit is expected to be slower, i.e., residence time is more than the other at a particular temperature, the effective residence time will be less than what is expected for the noninterdigitized alkyl chains. However, they being of the same order, it was not possible to obtain the two different residence times, which actually correspond to two dynamically different rotational units above 340 K.

AgC_{12}: The QENS experiment were carried out for the layered system, AgC_{12} as well. In this system only one transition is observed in DSC at 400 K where the Bragg peaks were found to disappear indicating melting of the lattice[13]. Spectra were recorded at 300, 340, 360, 380, 390, and 400 K. No QE broadening was observed below 400 K but it was seen at 400 K (Figure 8), which corroborates with the DSC data and therefore attributed to melting. Similar analysis as in the case of other systems described above, was performed and the elastic and QE parts were separated. The EISF extracted is shown in Figure 9; the fit captures the changes qualitatively. The rotational dynamics seems to be very similar in AgC_8 and AuC_{18}. All the chains contribute to the observed dynamical motion. The model $S(Q,\omega)$ assuming 6-fold jump diffusion model with radius of gyration 2.2 (±0.2) Å was found to give very good fit to the data over the whole Q range. The residence time found was 3.8 (±0.4) ps.

IV. Conclusions

Dynamics of alkyl chains in an isolated monolayer protected cluster, a superlattice of the cluster and a layered silver thiolate have been studied using the quasielastic neutron scattering technique. The most probable geometry of motions in all the three cases investigated were uniaxial rotations or $N \geq 6$ site jump diffusion. The residence time shows the level of dynamics. In AgC_8 solid, dynamics exist at room temperature but are limited by hindered rotations by neighboring alkyl chain interactions. As explained by neutron scattering data, about 50% of alkyl chains are dynamic at room temperature in the case of AgC_8. The contribution to the dynamical motion increases with temperature. At 340 and 360 K, 56 and 57% of the alkyl chains, respectively are found to be dynamic. At 380 K, which is close

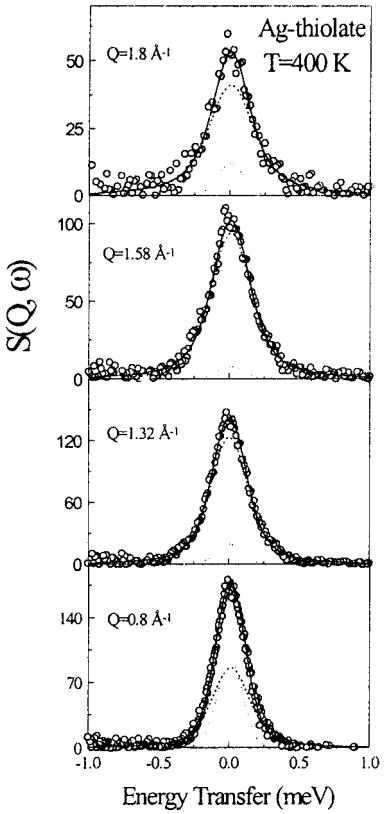

Figure 8. QENS spectra from layered Ag-thiolate (AgC_{12}) at $T = 400$ K at different Q values. Dashed and the dotted lines are the quasielastic and elastic components, respectively.

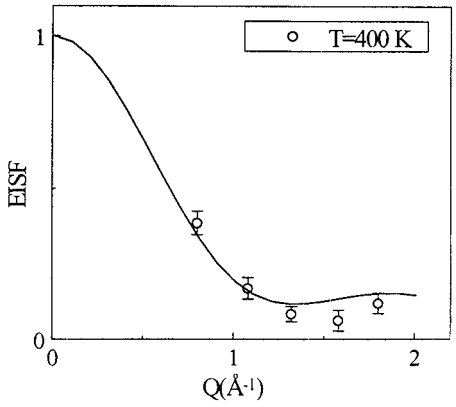

Figure 9. EISF as obtained for AgC_{12} at 400 K. The solid line corresponds to a model in which a particle performs random jumps among $N = 6$ equivalent sites on a circle with radius, a equal to 2.2 Å.

to the alkyl chain melting point all the chains are dynamic. In AuC_{18}, all the chains participate in rotations above the alkyl chain melting temperature, supporting the fact that superlattice structure is minimum in this case. The greater residence time when compared to AgC_8 at similar temperatures may be due to increased alkyl chain length limiting the rotational dynamics. This increase in residence time may also be indicative of the larger conformational order present in these systems. In AgC_{12}, the presence of rotational motion is seen only at and above 400 K, which is the outcome of increased packing factor and thus restricted dynamics. Observed dynamics in all the systems are solely due to the freedom of the alkyl chains. Thus the rotations of alkyl chain assemblies could be revealed and understood to a large extent by the neutron scattering models. We have shown that the studies performed so far on structure and properties of monolayers can be complemented with neutron scattering measurements. The study has provided definitive confirmations on, (1) the absence of measurable rotational dynamics in ordered alkyl chain assemblies such as in AuC_{18} at room temperature, (2) gradual evolution of the rotational motions with temperature, (3) increased interchain interactions inhibiting free rotations in superlattices compared to free clusters, and (4) absence of free rotations even up to 400 K in thiolates. We have observed distinct differences in the alkyl chain interactions in the superlattice and isolated clusters. This study has clearly shown that at least in longer chain thiolate protected clusters, the alkyl chains are conformationally frozen and room-temperature dynamics does not show up in the picosecond time scale. This is in contrast to the situation in 2D monolayers where the alkyl chains preserve rotational freedom and exist in the "rotator phase" at room temperature.[8] We have also shown that the alkyl chain assembly is more dense giving a shorter contact distance between the chains than that in the case of planar monolayers. Although reasons behind the differences between monolayers on gold and silver clusters are not understood at the moment, we hope that additional studies, being performed currently, looking at the dynamics as a function of chain length and as a function of monolayer functionality, will give more information pertaining to the molecular motions in these interesting nanophase materials.

Acknowledgment. The fruitful discussion with Dr. B. A. Dasannacharya is gratefully acknowledged. T.P. and B. N. are grateful to the Inter-University Consortium for DAE Facilities for financial support. The monolayer protected cluster research program at Chennai is supported by the Council for Scientific and Industrial Research, New Delhi. Mr. A. Balasundaram was involved in the early part of this work.

References and Notes

(1) Ulman, A. *An introduction to Ultrathin Organic Films from Langmuir−Blodgett to Self-Assembly*; Academic Press: New York, 1991.

(2) Roberts, G. (Ed.) *Langmuir−Blodgett Films*; Plenum Press: New York, 1990.

(3) Ulman, A. *Chem. Rev.* **1996**, *96*, 1533.

(4) (a) Sangiv, J. *J. Am. Chem. Soc.* **1980**, *102*, 92. (b) Ogawa, H.; Chihera, T.; Taya, K. *J. Am. Chem. Soc.* **1985**, *107*, 1365. (c) Nuzzo, R. G.; Allara, D. L. *J. Am. Chem. Soc.* **1983**, *105*, 4481. (d) Nuzzo, R. G.; Dubois, L. H.;.Allara, D. L *J. Am. Chem. Soc.* **1990**, *112*, 558. (e) Laibinis, P. E.; Whitesides, G. M.;.Allara, D. L.;Tao, Y.-T.; Parikh, A. N.; Nuzzo, R. G. *J. Am. Chem. Soc.* **1991**, *113*, 7152.

(5) (a) Poirier, G. E. *Chem. Rev.* **1997**, *97*, 1117. (b) Bain, C. D.; Troughton, E. B.; Tao, Y.-T.; Eoall , J.; Nuzzo , R. G. *J. Am. Chem. Soc.* **1989**, *111*, 321. (c) Nuzzo, R. G.; Zegarski, B. R.; Dubois, L. H. *J. Am. Chem. Soc.* **1987**, *109*, 733. (d) Nuzzo, R. G.; Fusco, F. A.; Allara, D. L. *J. Am. Chem. Soc.* **1987**, 109, 2358. (e) Allara, D. L. *Langmuir* **1986**, *2*, 239.

(6) Hostetler, M. J.; Murray, R. W. *Curr. Opin. Colloid Interface Sci.* **1997**, *2*, 42 and references therein.

(7) (a) Terril, R. H.; Postlethwaite, T. A.; Chen, C.-H.; Poon, C.-D.; Terzis, A.; Chen, A.; Hutchison, J. E.; Clark, M. R.; Wignall, G.; Londono, J. D.; Superfine, R.; Falvo, M.; Johnson, C. S., Jr.; Samulski, E. T.; Murray, R. W. *J. Am. Chem. Soc.* **1995**, *117*, 12537. (b) Badia, A.; Cuccia, L.; Demers, L.; Morin, F.; Lennox, R. B. *J. Am. Chem. Soc.* **1997**, *119*, 2682. (c) Hostler, M. J.; Stokes, J. J.; Murray, R. W. *Langmuir* **1996**, *12*, 3604.

(8) Dubois, L. H.; Nuzzo, R. G. *Annu. Rev. Phys. Chem.* **1992**, *43*, 437 and references therein.

(9) Whetten, R. L.;.Shaffigullin, M. N.; Khoury, J. T.; Schaaf , T. G.; Vezmar, I.; Alvarez, M. M.; Wilkinson, A. *Acc. Chem. Res.* **1999**, *32*, 397 and references therein.

(10) Sandhyarani, N.; Resmi, M. R.; Unnikrishnan, R.; Vidyasagar, K.; Shuguang, Ma; Antony, M. P.; Paneer Selvam, G.; Visalakshi, V.; Chandrakumar, N.; Pandian, K.; Tao, Y.-T.; Pradeep, T. *Chem. Mater.* **2000**, *12*, 104.

(11) Sandhyarani, N.; Pradeep, T.; Chakrabarthi, J.; Yousuf, M.; Sahu, H. K. *Phys. Rev. B* **2000**, *62*, R739.

(12) Sandhyarani, N.; Pradeep, T.; Antony, M. P.; Paneer Selvam, G. *J. Chem. Phys.* **2000**, *113*, 9794.

(13) Badia, A.; Singh, S.; Demers, L.; Cuccia, L.; Brown , G. R.; Lennox, R. B. *Chemistry−A European Journal* **1996**, *2*, 359.
(14) Dance, I. G.; Fisher, K. J.; Herath Bamda, R. M.; Scudder, M. L. *Inorg. Chem.* **1991**, *30*, 183.
(15) Parikh, A. N.; Gillmor, S. D.; Beers, J. D.; Beardmore, K. M.; Cutts, R. W.; Swanson, B. I. *J. Phys. Chem*. **1999**, *103*, 2850. (b) Bansebaa, F.; Ellis, T. H.; Kruus, E.; Voicu, R.; Zhou, Y. *Langmuir* **1998**, *14*, 6579.
(16) Luedtke, W. D.; Landman, U. *J. Phy. Chem*. **1996**, *100*, 13323.
(17) Markichev et al., *Phys. B* **1994**, *198*, 197.
(18) Dubois, E.; Perzynski, R.; Boue, F.; Cabuil, V. *Langmuir* **2000**, *16*, 5617.
(19) Hjelm R. P.; Schteingart, C. D.; Hofmann, A. F.; Thiyagarajan, P. *J. Phys. Chem. B* **2000**, 104, 197.
(20) Lutterbach, N.; Versmold, Reus, V.; Belloni, L.; Zemb, Th., Lindner, P. *Langmuir* **1999**, 15, 345.
(21) Bee, M. *Quasielastic Neutron Scattering*; Adam-Hilger: Bristol, 1988.
(22) Press: W. *Single Particle Rotations in Molecular Crystals*: Springer: Berlin, 1981.
(23) Mukhopadhyay, R., Goyal, P. S.; Carlile, C. J. *Phys. Rev. B* **1993**, *48*, 2880.
(24) Mukhopadhyay, R.; Mitra, S.; Tsukushi I.; Ikeda, S. *Chem. Phys. Lett.* **2001**, *341*, 45. (b) Mitra, S.; Mukhopadhyay, R.; Venu, K. *Chem. Phys*. **2000**, *261*, 149. (c) Mitra, S.; Mukhopadhyay, R.; Tsukushi I.; Ikeda, S. *J. Phys.*: *Condens. Matter* **2001**, *13*, 8455.
(25) Mukhopadhyay, R.; Mitra, S.; Paranjpe S. K.; Dasannacharya, B. A. *Nucl. Instrum. Methods A* **2001**, *474*, 45. (b) Dasannacharya, B. A. *Phys. B* **1992**, *180/181*, 880.
(26) Mukhopadhyay, R.; Dasannacharya, B. A. *BARC Rep.* **1985**, I-755.
(27) Kjems, J. K.; Reynolds, P. A. IAEA-SM-155/F-4, 1972.
(28) Barnes, J. D. *J. Chem. Phys.* 1973, *58*, 5193.
(29) Dianoux, A. J.; Volino, F.; Hervet, H. *Mol. Phys*. 1975, *30*, 1181.
(30) Sears, V. F. *Can. J. Phys.* 1966, *44*, 1299.